Proc. of 17th Int. Display Workshop (IDW '10), vol. 2, Fukuoka, pp.1237-1240(2010.12.1), Invited paper.

Spatial Imaging Based on Extremely High-Definition Computational Holography

— Wave-Field Oriented 3D imaging —

Kyoji Matsushima

Department of Electrical and Electronic Engineering, Kansai University,
3-3-35 Yamate-cho, Suita, Osaka 564-8680, Japan

ABSTRACT

Extremely high-definition displays beyond Super Hi-Vision give us a new horizon in the field of 3D imaging. This paper introduces spatial 3D imaging brought by computational holography and techniques for numerical propagation of wave-fields that make it possible to create the spatial 3D images.

1. INTRODUCTION

The resolution of display devices increases year by year. The pixel density of the devices also increases with increase of the display resolution. In current display devices, we can treat light as a ray. However, we will have a difficulty in handling light by using conventional ray-optics beyond the Super Hi-Vision.

The phenomenon of diffraction governs the behavior of light of display devices in the pixel resolution less than 1 μm at a rough estimate. In this case, we need techniques for simulating field propagation based on wave optics to predict what is seen in the display screen. Many researchers and suppliers of the display devices may believe that such kind of high-definition is unnecessary. However, let me emphasize that the high definition gives us a new horizon; that is spatial imaging. The spatial imaging is one of 3D imaging technologies, but the principle and the reconstructed 3D image are fundamentally different from conventional 3D images.

In this article, some techniques for field propagation in a free space are presented for numerical simulation of diffraction. Furthermore, the spatial imaging by computational holography based on the field propagation is introduced as a novel technology of 3D imaging.

2. WAVE-FIELD PROPAGATION

Wave-fields diffracted by display devices propagate in a free space. Then, we observe the field intensity by our eye. Thus, numerical techniques for simulating field propagation play an important role in the spatial imaging.

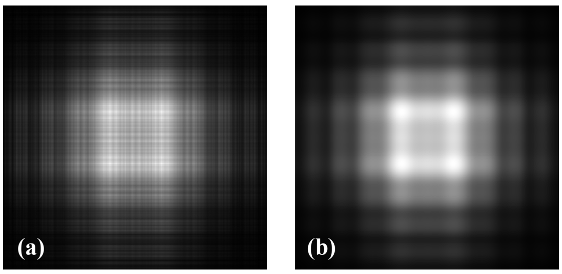

Fig. 1 Diffraction by a rectangular aperture [3]
Amplitude images calculated by:
(a) The conventional AS [2] and (b) improved BL-AS [3].

2.1 Propagation between Parallel Planes

The common category of free-space propagation is propagation between parallel planes [1]. In this category, various methods such as the single Fourier-transform-based Fresnel method (SFT-FR) and the convolution-based Fresnel method are continually being proposed. However, the angular spectrum-based method (AS) [2] is potentially the most powerful, because it is rigorously derived from the Rayleigh-Sommerfeld integral. However, the traditional AS cannot serve as an all-round method in a numerical implementation due to sampling problems. The author recently proposed the band-limited AS (BL-AS) to avoid the sampling problems [3]. This is a simple, yet effective, improvement of the AS that magnifies the range of the effective propagation distance of the AS, as shown in Fig. 1.

2.2 Propagation between non-Parallel Planes

Another category of free space propagation is propagation between non-parallel planes. The AS also plays an important role in this category. The rotational transformation of wave

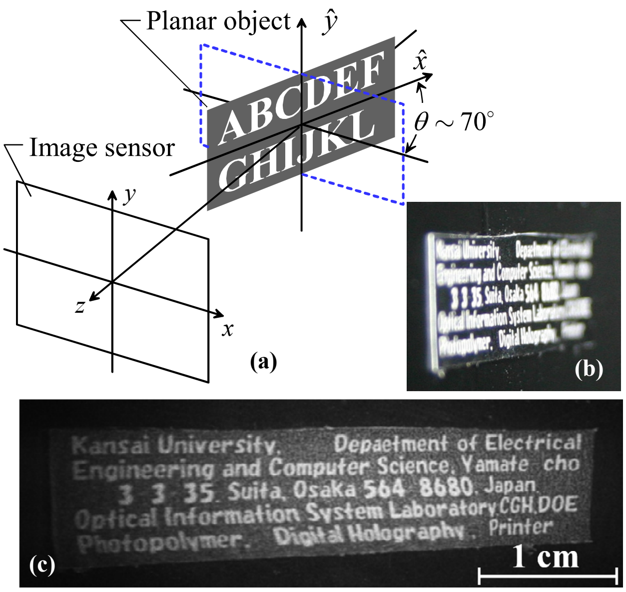

Fig. 2 Clear imaging of deeply tilted surface [5]
(a) Capturing the wave-field by digital holography
(b) A close-up photograph of the planar object
(c) The amplitude image obtained by using the rotational transformation

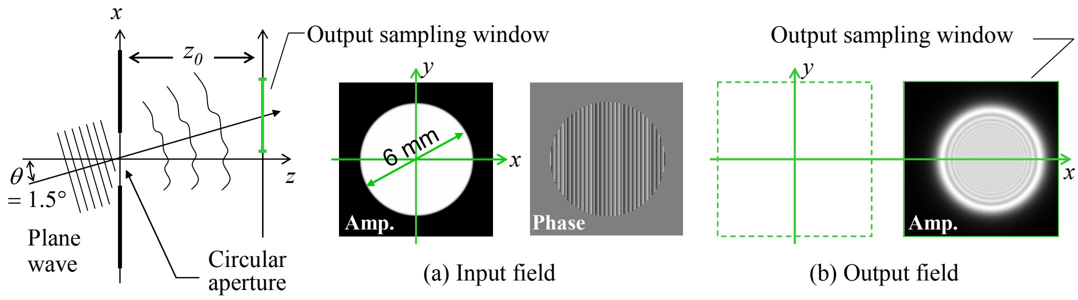

Fig. 3 Simulation of diffraction by a circular aperture with the incident plane wave travelling in an off-axis direction [7]
(a) Input field of simulation, (b) Diffraction image numerically calculated by using the Shift-AS

fields [4,5], formulated as an expansion of the AS, makes it possible to calculate wave fields in arbitrarily tilted planes from a given source field. This method is used for clear imaging of deeply tilted surfaces [5], as shown in Fig. 2.

2.3 Off-Axis Numerical Propagation

Recently, a new category of free space propagation, off-axis numerical propagation, was added to the field. This involves propagation between parallel planes, but with the sampling window of the output destination field shifted from that of the input source field. This is very useful in cases where a field is not paraxial and travels in an off-axis direction. The most notable method for off-axis numerical propagation is the shifted Fresnel method (Shift-FR) [6]. This excellent technique is derived from the SFT-FR using a scaled FFT. However, the Shift-FR has a serious problem of strong aliasing in short distance propagation.

A novel method for resolving the problem, called the shifted angular spectrum method (Shift-AS) [7], has been proposed as a generalization of the BL-AS. Figure 3 (b) shows amplitude distribution of a wave-field simulated by the Shift-AS. The wave-field is a plane wave travelling at the incident angle of θ= 1.5°, diffracted by a circular aperture of 6 mm in diameter, as in (a). In conventional propagation methods, calculation of the diffracted fields in planes far from the aperture requires much computational effort (computation time and memory), because the diffracted field becomes more distant from the optical axis in proportion to propagation distance. In such cases, the sampling window needs to be expanded in conventional methods. This problem is solved by using the Shift-AS, as in (b).

3. COMPUTATIONAL HOLOGRAPHY

3.1 Introduction to Computer-Generated Hologram

As is well-known in the principle of holography, the wave-field emitted from an object can be recorded by interference of a reference field. The recorded object field is reconstructed by diffraction by the interference fringe pattern. Therefore, if we can generate the fringe pattern, any object field, even if the object is not real-existent, can be reconstructed. This fringe pattern is called Computer-Generated Hologram (CGH).

Since the reference field is generally given by simple mathematical expression, only synthesis of the object field from its numerical model is necessary for generating the fringe pattern. The point-based method has been used for numerical synthesis of object fields for a long time. However, the point-based methods are much time-consuming especially in creation of full-parallax CGHs for surface-modeled objects. Therefore, the polygon-based method was recently presented for overcoming the problem [8].

3.2 The Polygon-Based Method for Surface Object

3.2.1 Theoretical model of a polygonal surface

We can see real objects illuminated by a light source, because the object surfaces scatter the light, as shown in Fig. 4 (a). Suppose that an object is composed of many polygonal planes (polygons) and each polygon emits the wave-field. This field is similar to that diffracted by the aperture irradiated by a plane wave, as in (b). The aperture has the same shape and slant as the polygon. However, a simple polygonal aperture

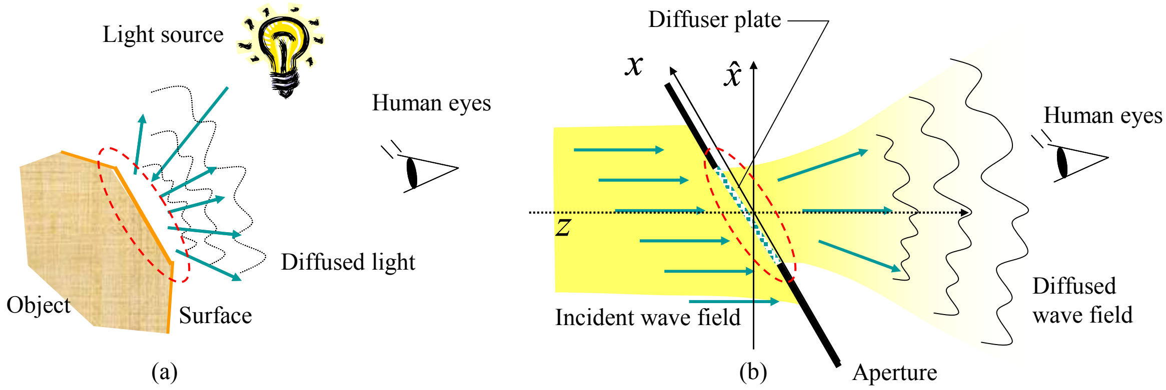

Fig. 4 The theoretical model of a polygonal surface
(a) The visible surface of a real object, (b) Diffuser-mounted aperture for imitating the visible surface

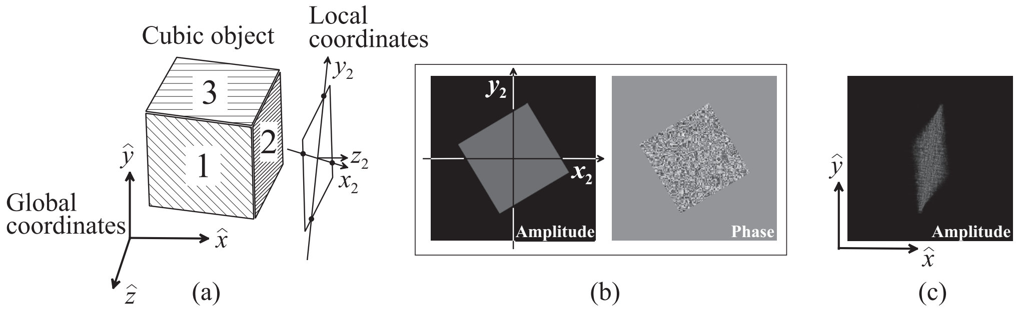

Fig. 5 The principle for synthesizing object field by the polygon-based method
(a) The numerical model of a surface object, (b) The surface function for the polygon #2, (c) The polygon field of the polygon #2

may not behave as if it is a surface source of light, because the aperture size is too large to diffract incident light, and thus light passing through the aperture is not diffused. Therefore, the polygonal surface source is imitated by a virtual (numerical) diffuser that is mounted in the aperture whose shape and tilt angle correspond with the polygon.

3.2.2 Surface functions

To compute the wave-field diffracted by the diffuser with a polygonal shape, a surface function is provided for each individual polygon in the local coordinate system that is also specific to the polygon. An example of the surface function is shown in Fig. 5 (b).

The surface function $h(x,y)$ for a polygon is generally given in the following form:

$$h(x,y) = a(x,y)\exp[i\phi(x,y)],$$

where $a(x,y)$ and $\phi(x,y)$ are the real-valued amplitude and phase distribution in the local coordinates. The phase pattern $\phi(x,y)$ is not visible in principle, because all image sensors including human retinas can detect only the intensity of light, whereas the amplitude pattern $a(x,y)$ directly determines the appearance of the polygon. Therefore, while the properties required for the diffuser should be provided by the phase pattern,

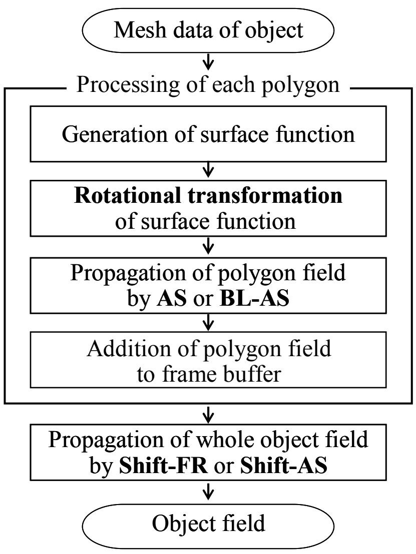

Fig. 6 The procedure for calculating the object field by using the methods for wave-field propagation

the shape, shade and texture of the polygon are given by the amplitude pattern.

3.2.2 Calculation of object fields

The procedure for calculation of object fields is shown in Fig. 6. The surface function of a polygon is yielded from the vertex data of the polygon. Since the surface function is given in a plane not parallel to the hologram, the rotational transformation is used in order to calculate the polygon field in the parallel plane, as shown in Fig.5 (c). Then, the polygon field is propagated shortly by using AS or BL-AS in order to gather all polygon fields in a plane and accumulated in a single frame buffer. This plane is called the object plane.

The polygon fields gathered in the object plane should be propagated to the hologram or the plane of a silhouette mask, as described in the following section. However, the fame buffer for the whole object field is commonly too large to simultaneously store in memory. Therefore the field is segmented and propagated by using off-axis numerical propagation such as the Shift-FR or Shift-AS [9].

3.3 The Silhouette Method for Light-Shielding

Occlusion is one of the most important mechanisms in the perception of 3D scenes. To reconstruct occluded 3D scenes, light behind an obstacle must be shielded by the obstacle.

Supposing that a background wave-field emitted from other objects behind the obstacle is given in the object plane. In the silhouette method [9, 10], the background wave-field is

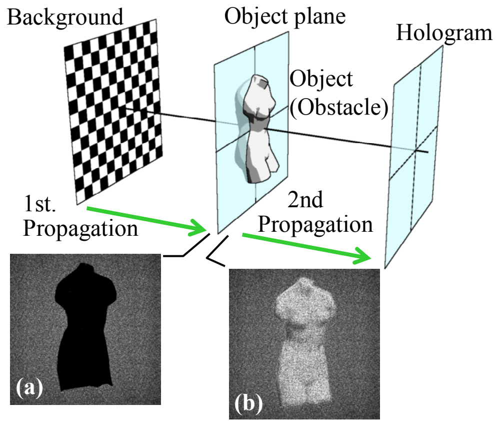

Fig. 7 Silhouette masking of the background field [9]
(a) The background field masked by the object silhouette
(b) The object field superimposed on the masked field

masked with the shape of the silhouette of the obstacle, as shown in Fig. 7 (a). Then, the wave-field of the obstacle itself is superimposed on the masked background wave-field in the object plane, as in (b). This combined wave-field is again propagated onto the next object or the hologram plane.

4. HIGH-DEFINITION CGH

4.1 Calculation

The size and viewing-angle of CGHs are the most important parameters for reconstructing high-quality 3D images. Since a large viewing-angle requires high spatial resolution in CGHs, both lead to an extremely large number of pixels for CGHs in that the frame buffer usually can not be stored simultaneously in main memory. Therefore, the frame buffer must be segmented and the wave-field must be numerically propagated by using methods for off-axis numerical propagation such as Shift-AS or Shift-FR [9].

4.2 Optical Reconstruction

Figures 7 and 8 are photographs of optical reconstruction of high-definition CGHs as examples. Number of pixels of these CGHs reaches to 8 G pixels and the viewing-angles are approximately 46° in horizontal and 37° in vertical. These extremely high-definition CGHs give viewers a strong sensation of depth and reality that are never provided by conventional 3D systems [11].

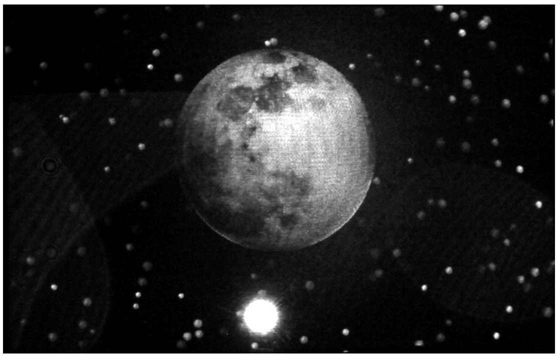

Fig. 7 Optical reconstruction of "The Moon"
Sizes: 131,072 × 65,536 pixels, Pitches: 0.8 μm × 1.0 μm
Viewing-angle: 46° × 37°

5. CONCLUSION

Extremely high-definition displays make it possible to produce the light of the object itself. It is a true 3D image based on wave-field propagation. This spatial image never has been created by current 3D systems that give only binocular disparity [12].

ACKNOWLEDGEMENT

I would like to thank Prof. Nakahara for fabrication of CGHs and Mr. Nakamura for assistance in formulation and calculation. This work was supported by the JSPS.KAKENHI (21500114).

REFERENCES

[1] T. M. Kreis, M. Adams, and W. P. O. Jüptner, "Methods of digital holography: A comparison," SPIE Proc. **3098**, 224–233 (1997).

[2] J. W. Goodman, *Introduction to Fourier Optics*, 2nd ed. (McGraw-Hill, 1996), chap. 3.10.

[3] K. Matsushima and T. Shimobaba, "Band-limited angular spectrum method for numerical simulation of free-space propagation in far and near fields," Opt. Express **17**, 19662-19673 (2009).

[4] K. Matsushima, H. Schimmel, and F. Wyrowski, "Fast calculation method for optical diffraction on tilted planes by use of the angular spectrum of plane waves," J. Opt. Soc. Am. **A20**, 1755–1762 (2003)

[5] K. Matsushima, "Formulation of the rotational transformation of wave fields and their application to digital holography," Appl. Opt. **47**, D110–D116 (2008).

[6] R. P. Muffoletto, J. M. Tyler, and J. E. Tohline, "Shifted Fresnel diffraction for computational holography," Opt. Express **15**, 5631–5640 (2007).

[7] K. Matsushima, "Shifted angular spectrum method for off-axis numerical propagation," Opt. Express **18**, 18453-18463 (2010).

[8] K. Matsushima, "Computer-generated holograms for three-dimensional surface objects with shade and texture," Appl. Opt. **44**, 4607–4614 (2005).

[9] K. Matsushima and S. Nakahara, "Extremely high-definition full-parallax computer-generated hologram created by the polygon-based method," Appl. Opt. **48**, H54-H63 (2009)

[10] A. Kondoh and K. Matsushima, "Hidden surface removal in full-parallax CGHs by silhouette approximation," Systems and Computers in Japan **38**, 53–61 (2004).

[11] K. Matsushima, M. Nakamura, S. Nakahara, I. Kanaya, "Computational Holography: Real 3D by Fast Wave-Field Rendering in Ultra-High Resolution," SIGGRAPH 2010, Los Angeles, 77B (2010).

[12] http://www.youtube.com/watch?v=DdOveIue3sc

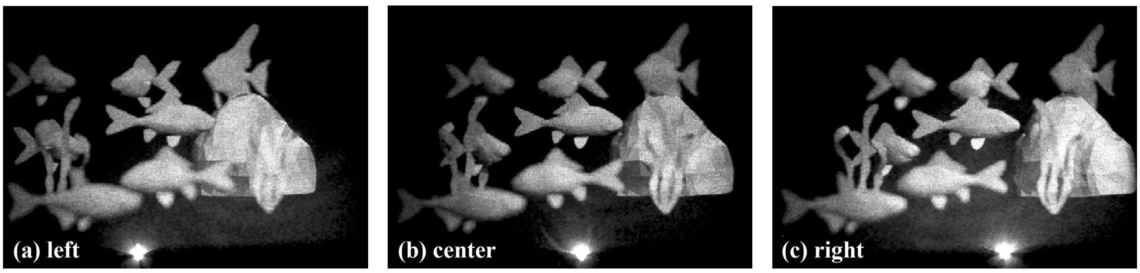

Fig. 8 Optical reconstruction of "Aqua 2"
Photographs are taken from different angles.
Sizes: 131,072 × 65,536 pixels, Pitches: 0.8 μm × 1.0 μm, Viewing-angle: 46° × 37°